Original Article

Lightwave-reinforced stem cells with enhanced wound healing efficacy

Journal of Tissue Engineering
Volume 12: 1–16

DOI: 10.1177/20417314211067004
journals.sagepub.com/home/tej
SAGE

Yu-Jin Kim[1]*, Hye Ran Jeon[2,3]*, Sung-Won Kim[1], Yeong Hwan Kim[1], Gwang-Bum Im[1], Jisoo Im[1], Soong Ho Um[1], Sung Min Cho[1], Ju-Ro Lee[4], Han Young Kim[5], Yoon Ki Joung[4,6], Dong-Ik Kim[2,3] and Suk Ho Bhang[1]

Abstract

Comprehensive research has led to significant preclinical outcomes in modified human adipose-derived mesenchymal stem cells (hADSCs). Photobiomodulation (PBM), a technique to enhance the cellular capacity of stem cells, has attracted considerable attention owing to its effectiveness and safety. Here, we suggest a red organic light-emitting diode (OLED)-based PBM strategy to augment the therapeutic efficacy of hADSCs. In vitro assessments revealed that hADSCs basked in red OLED light exhibited enhanced angiogenesis, cell adhesion, and migration compared to naïve hADSCs. We demonstrated that the enhancement of cellular capacity was due to an increased level of intracellular reactive oxygen species. Furthermore, accelerated healing and regulated inflammatory response was observed in mice transplanted with red light-basked hADSCs. Overall, our findings suggest that OLED-based PBM may be an easily accessible and attractive approach for tissue regeneration that can be applied to various clinical stem cell therapies.

Keywords

Photobiomodulation, human adipose-derived stem cells, wound healing, angiogenesis

Date received: 13 October 2021; accepted: 29 November 2021

Introduction

Photobiomodulation (PBM), also known as low-level light/laser therapy or low-level light irradiation, is noninvasive, effective, nontoxic, and has been clinically applied for various purposes owing to its therapeutic properties.[1–6] In various studies, PBM has been shown to reduce pain and inflammation and it is also used to treat diseases such as edema, acne, dermatitis, ulcers, burns, and arthritis.[2,5,7–14] As light sources, coherent light (laser) or noncoherent light (light-emitting diode, LED) are generally used.[1–4] Despite the continuous development in light sources, there remains a concern of heat damage, and a proper heat sink is required.[3,15] Furthermore, previous studies have been conducted with customized LED-based devices.[16–18] Clinical LED devices based on point light sources have been reported to show unsatisfactory results due to nonuniform irradiation and difficulty in applying them to large lesions.[2] Moreover, light irradiation parameters, such as wavelength, fluence (J/cm^2), irradiance (mW/cm^2), and radiation time, need to be established and optimized. Since the conditions previously reported vary widely, there is no standardization.[1–4]

[1]School of Chemical Engineering, Sungkyunkwan University, Suwon, Gyeonggi-do, Republic of Korea
[2]Department of Health Sciences and Technology, SAIHST, Sungkyunkwan University, Gangnam-gu, Seoul, Republic of Korea
[3]Division of Vascular Surgery, Samsung Medical Center, Sungkyunkwan University School of Medicine, Gangnam-gu, Seoul, Republic of Korea
[4]Center for Biomaterials, Biomedical Research Institute, Korea Institute of Science and Technology, Seoungbuk-gu, Seoul, Republic of Korea
[5]Department of Biomedical-Chemical Engineering, The Catholic University of Korea, Bucheon, Gyeonggi, Republic of Korea
[6]Division of Bio-Medical Science & Technology, University of Science and Technology, Yuseong-gu, Daejeon, Republic of Korea

*These authors contributed equally to this work.

Corresponding authors:
Dong-Ik Kim, Department of Health Sciences and Technology, SAIHST, Sungkyunkwan University, Gangnam-gu, Seoul 06355, Republic of Korea, Division of Vascular Surgery, Samsung Medical Center, Sungkyunkwan University School of Medicine, Gangnam-gu, Seoul 06351, Republic of Korea.
Email: dikim@skku.edu

Suk Ho Bhang, School of Chemical Engineering, Sungkyunkwan University, 2066, Seobu-ro, Jangan-gu, Suwon, Gyeonggi-do 16419, Republic of Korea.
Email: sukhobhang@skku.edu

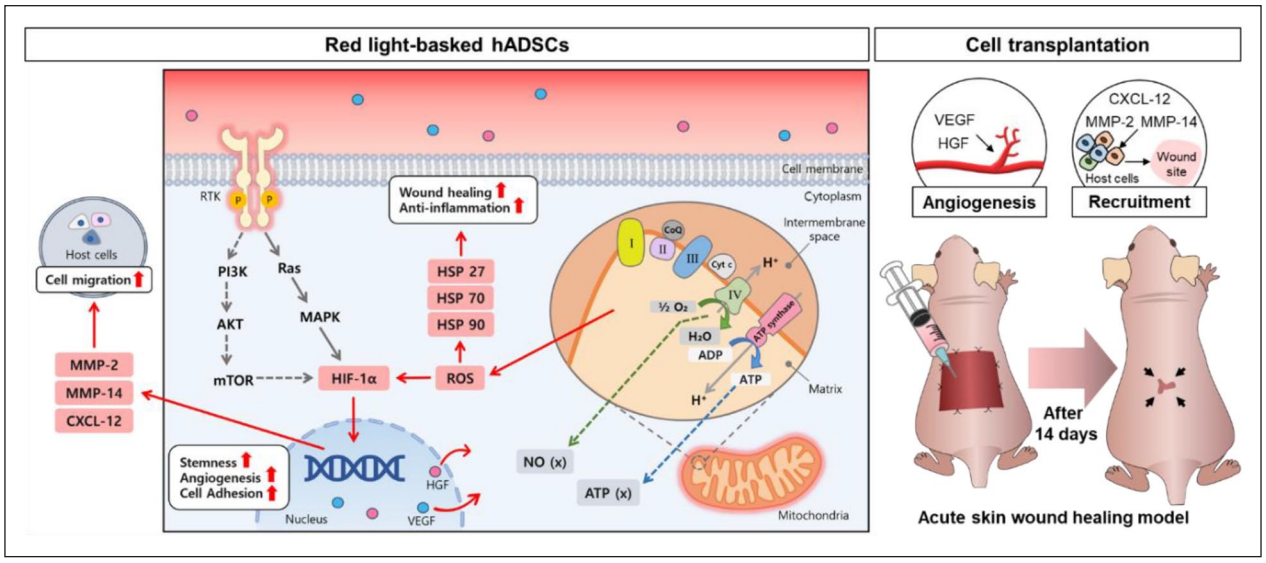

Figure 1. Schematic illustration of red organic light-emitting diode (OLED) light-basked human adipose-derived mesenchymal stem cells (hADSCs) for effective wound healing. Cellular capacities of hADSCs basked with red OLED light (B_RL) were enhanced in terms of angiogenesis, cell adhesion, migration, and stemness.

Most studies on the wound healing effect, using lasers and LEDs, have demonstrated that PBM stimulates the proliferation and migration of various types of cells, including mesenchymal stem cells (MSCs), and promotes angiogenesis, expression of growth factors, and production of collagen, which helps wound healing.[2,3,6,14,17,19] The mechanism of PBM has not yet been fully elucidated. However, the commonly theorized mechanism is that photons of light are absorbed by the enzyme cytochrome c oxidase (CCO), which acts as a primary photoreceptor in complex IV of the mitochondrial respiratory chain.[2,4,6] As a result, the mitochondrial membrane potential is increased, and nitric oxide (NO) is photodissociated from the heme iron and copper center of CCO. In turn, the synthesis of adenosine triphosphate (ATP) and the production of mild reactive oxygen species (ROS) are increased. By altering the cellular redox state, PBM can regulate the numerous intracellular signaling pathways that lead to the enhancement of cellular function.[2,4,6] In the referenced studies, even though similar wavelengths were used, the range of irradiation time was wide, from seconds to hours, and irradiation was repeated according to the experimental conditions.[14,20–22] Therefore, a commercially available light source that could maintain the effect of PBM for a long time and establishing optimized conditions for irradiation are required.

In this study, we suggest that PBM using organic light-emitting diodes (OLEDs) guarantees therapeutic effects through specific molecular mechanisms and increased angiogenic efficiency of hADSCs. Although OLEDs are expensive and have a short lifetime for high-quality light, it is an alternative device that can overcome the limitations of laser and LED.[23,24] OLEDs are more useful because of their safety, high efficiency, low power consumption, and lack of overheating. In particular, unlike LEDs or lasers, OLEDs are surface light sources that can uniformly distribute light over a wide area. Recently, some research teams have applied OLEDs to PBM and confirmed the effects of improved cellular function and wound healing.[25,26] However, the effect has yet to be proven by applying OLED-based PBM to stem cells, which are considered an attractive source in the tissue engineering field and have various advantages as effective therapeutics.

We investigated the influence of OLEDs, with established parameters, on cellular function and angiogenesis in hADSCs, and confirmed wound closure efficacy in a mouse wound healing model (Figure 1). The red light irradiation was applied for 24 h to hADSCs. To observe the cellular behavioral changes, the red light irradiated hADSC samples were collected between 0 and 48 h after the 24 h irradiation. When hADSCs were basked with the red OLED light (B_RL), temperature of the medium in which the cells were cultured and the expression of heat shock proteins (HSP27, HSP70, HSP90α) were monitored to determine whether there was heat damage. Since there was no significant difference in temperature, ROS was identified as a factor affecting HSP expression. We found that enhancement of stemness, cell migration, and adhesion ability, and maintenance of cell viability. Subsequently, we conducted in vitro and in vivo experiments to demonstrate whether PBM using OLEDs promotes angiogenesis and the wound healing effect. Generally, wound healing is multiple processes (hemostasis, inflammation, cell proliferation, and tissue remodeling), which involve high

expression levels of anti-inflammatory cytokines and growth factors. Previous studies have shown that the wound healing was effective in animal models by controlling inflammation, promoting collagen deposition, and vascularization through the regulation of various factors expression.[27–34] Especially angiogenesis is a necessary process for enhancing blood flow and forming extracellular matrix microenvironment formation.[35,36] Therefore, we hypothesized that the increased expression of factors related to angiogenesis in hADSCs via OLED-based PBM would accelerate wound closure compared to that in hADSCs without light irradiation. We applied commercially available OLED-based PBM to stem cells under optimized parameters and suggested an original technology that can be applied to wound treatment using stem cells and cell therapy research in the future.

Methods

Reagents and antibodies

The following antibodies were used for western blot analysis and immunofluorescence staining: anti-BCL2 (1:500, Abcam, Cambridge, MA, USA), anti-KLF4(1:500, Abcam), anti-SOX2 (1:500, Abcam), anti-NANOG (1:200, Abcam), anti-CASPASE3 (1:1000, Cell Signaling Technology, Danvers, MA, USA), anti-MMP2 (1:1000, Cell Signaling Technology), anti-MMP14 (1:1000, Cell Signaling Technology), anti-Laminin (1:1000, Abcam), anti-involucrin (1:500, Abcam), anti-col I (1:1000, Abcam), anti-beta actin (1:5000, Sigma-Aldrich, St. Louis, MO, USA), goat anti-mouse IgG-HRP (1:5000), and rabbit IgG-HRP (1:10,000, Bethyl Laboratories, Montgomery, TX, USA).

Cell culture and basking in red light using OLED

hADSCs were purchased from Lonza (Walkersville, MD, USA) and cultured in cell culture dishes (Corning, Steuben, NY, USA) with Dulbecco's modified Eagle's medium (DMEM; Gibco BRL, Gaithersburg, MD, USA), supplemented with 10% (v/v) fetal bovine serum (FBS; Gibco BRL) and 1% (v/v) penicillin-streptomycin (PS; Gibco BRL), in a 5% carbon dioxide (CO_2) cell incubator at 37°C. The culture medium was changed every second day. The hADSCs at passages 4–7 were used in the experiments. One day after seeding, the culture medium was replaced with fresh medium, and the cells were incubated with red OLED for 24 h. The red OLED was located under the dishes, and the gap between the OLED and the dishes was approximately 1 cm. Temperature of the culture medium was recorded immediately after irradiation using an infrared thermal imaging system (FLIR i2, FLIR Systems Inc., Wilsonville, OR, USA).

Quantitative reverse transcription-PCR (qRT-PCR)

TRIzol (Ambion, Austin, TX, USA), chloroform (Sigma-Aldrich), and 75% (v/v) ethanol (Sigma-Aldrich, in water) were used to isolate total RNA from cells according to the manufacturer's instructions. Reverse transcription was performed using 1.5 μg of pure total RNA and the Primescript RT Master Mix (TaKaRa, Kusatsu, Japan) to synthesize complementary DNA. The SsoAdvanced Universal SYBR Green Supermix (Bio-Rad, Hercules, CA, USA) and CFX Connect™ Real-time PCR Detection System (Bio-Rad) were used for qRT-PCR. The relative expression level was analyzed using the $2^{(-\Delta\Delta^{CT})}$ method.[37] Glyceraldehyde 3-phosphate dehydrogenase (*GAPDH*, in vitro) and beta-actin (β-*actin*, in vivo) served as the internal controls.

Intracellular ROS staining and analysis

2′,7-dichlorodihydrofluorescein diacetate (DCF-DA) (D339, Invitrogen, Carlsbad, CA, USA), a fluorescent indicator of ROS, was used to stain intracellular ROS. After basking in red light, the cells were incubated with 10 μmol/L DCF in phosphate-buffered saline (PBS; Gibco BRL) for 20 min at 37°C. After incubation, the cells were washed twice with PBS and observed under a fluorescence microscope (DFC 3000 G, Leica, Wetzlar, Germany). The concentration of intracellular ROS was determined by measuring the fluorescence intensity (Ex/Em of 494/524 nm) using a microplate reader (Varioskan LUX multimode microplate reader, Thermo Fisher Scientific, Waltham, MA, USA).

Live/dead staining

The live/dead assay was performed using fluorescein diacetate (FDA, 1.5 mg/mL in acetone; Sigma-Aldrich) and ethidium bromide (EB, 1 mg/mL in PBS; Sigma-Aldrich). FDA and EB stain the cytoplasm of viable cells green and the nuclei of nonviable cells red, respectively. The hADSCs were then treated with the staining solution for 5 min at 37°C. Following staining, the cells were washed thrice with PBS and observed under a fluorescence microscope (Leica).

Western blot analysis

Protein samples were prepared by extracting cells or tissues in RIPA buffer (Sigma-Aldrich). The Bradford reagent was used to quantify protein concentration (Bio-Rad). Proteins were boiled at 100°C for 10 min in 4× Laemmli sample buffer (Bio-Rad) containing β-mercaptoethanol, and the equivalent amounts of protein were loaded onto an 10% SDS-PAGE gel. Separated proteins were transferred onto nitrocellulose membranes and blocked with 1× TBS-T, containing 5% skim milk, for 1 h at room temperature (RT).

The membranes were incubated overnight with primary antibodies, then washed with 1× TBS-T and incubated with secondary antibodies for 1 h at room temperature (RT). Following TBS-T washes, protein bands were visualized using the ECL reagent WESTSAVE UP (ABfrontier, Seoul, Korea), and the membranes were exposed to X-ray films. The Image J software (National Institutes of Health, Bethesda, MD, USA) was used to analyze the expression of bands. Beta-actin (in vitro) and GAPDH (in vivo) were used as internal controls.

Cell adhesion analysis

For the re-adhesion test, untreated or B_RL-treated hADSCs were dissociated using trypsin-EDTA (Gibco BRL), and then the cells were reseeded in cell culture plates. Following 3 h of incubation under normoxia or hypoxia (2% O_2), the plates were washed with PBS to remove the unattached cells. The adherent cells were fixed with 4% paraformaldehyde (PFA; 10 min, RT). Cell membranes were stained with 1,1′-dioctadecyl-3,3,3′3′-tetramethylindocarbocyanine perchlorate (DiI; Sigma-Aldrich) according to the manufacturer's instructions. Nuclei were counterstained with 4,6-diamidino-2-phenylindole (DAPI; Vector Laboratories, Burlingame, CA, USA) and observed under a fluorescence microscope (Leica). The relative cell adhesion rate of the cells following treatment was examined in 24-well plates (2×10^4 cells/well) using the Cell Counting Kit-8 (CCK-8; Dojindo Molecular Technologies, Inc., Kumamoto, Japan). The cells incubated without OLED treatment served as the control group. Two hours after incubation with the CCK-8 solution at 37°C, the optical density (OD) of each well was measured at 450 nm using a microplate reader (Tecan, Mannedorf, Switzerland).

Cell scratch migration assay

To perform the cell scratch migration assay, hADSCs were cultured in 6-well plates until they reached confluence. After the cells were exposed to red light, the cell monolayer was scratched with a sterile 1000 μL tip (Neptune Scientific, San Diego, CA, USA) to create a linear gap. The floating cells were removed by washing with PBS (Gibco BRL). Cell migration was examined under a microscope equipped for 48 h. The relative migration area was calculated as [(original scratched area − remaining scratched area)/original scratched area] × 100%.[38]

Angiogenesis antibody array

To analyze angiogenesis-related protein expression in hADSCs, we used the Proteome Profiler Human Angiogenesis Array kit (R&D Systems, Minneapolis, MN, USA) according to the manufacturer's instructions. Briefly, all reagents and protein samples were prepared, 100 μg of cell lysate protein was used, and the membrane was blocked and the buffer aspirated. The antibody/sample mixture was added to the membrane and incubated overnight at 4°C. The next day, the membrane was washed with wash buffer and incubated with streptavidin-HRP for 30 min. After washing with wash buffer again, Chemi reagent was added, and the membrane was exposed to X-rays. Pixel density was quantified using the Image J software (National Institutes of Health) in each spot, and the average signal was calculated for duplicate spots.

Angiogenesis assay

Endothelial cell tube formation assay was performed using an in vitro angiogenesis assay kit (ab204726, Abcam) in accordance with the manufacturer's instructions. In brief, HUVECs were seeded onto an extracellular matrix gel (2×10^4 cells per well) in 100 μL of sample medium and incubated for 12 h at 37°C. Following incubation, the HUVECs were stained with a dye for 30 min at 37°C and observed under a fluorescence microscope (Leica).

ELISA

To analyze the secretion of angiogenic paracrine factors from hADSCs, we used ELISA kits for human VEGF human HGF (R&D Systems), according to the manufacturer's instructions. The conditioned medium was collected after 72 h of treatment with red OLED. The OD value of each well was measured at 450 nm using a microplate reader (correction 540 nm, Tecan).

Skin wound healing

Athymic mice (6 weeks old, 20 g of body weight, Orient Bio Inc., Sungnam, Korea) were anesthetized via intraperitoneal injection of xylazine (10 mg/kg) and ketamine (100 mg/kg). The mid-dorsal area of the skin of each mouse was incised to make a full-thickness skin wound ($2.0 \times 2.0\,cm^2$).[39,40] All animal treatments and experimental procedures were approved by the Institutional Animal Care and Use Committee of SKKU (SKKUIACUC2020-06-11-1). Mice with skin wounds were randomly divided into three experimental groups ($n = 5$ per group): no treatment (Tegaderm™ group, T), 0.5×10^6 hADSCs per mouse (cell + Tegaderm™ group, C@T), and 0.5×10^6 hADSCs per mouse (B_RL cell + Tegaderm™ group, B_RL C@T). The T group received no wound treatment, acting as the negative control (T), and the hADSCs were injected into the wound sites of the experimental animals. Briefly, hADSCs were subcutaneously injected at the edges of the wound (eight injections, 25 μL per site). All groups were treated with Tegaderm™ (3M Health Care, St. Paul, MN,

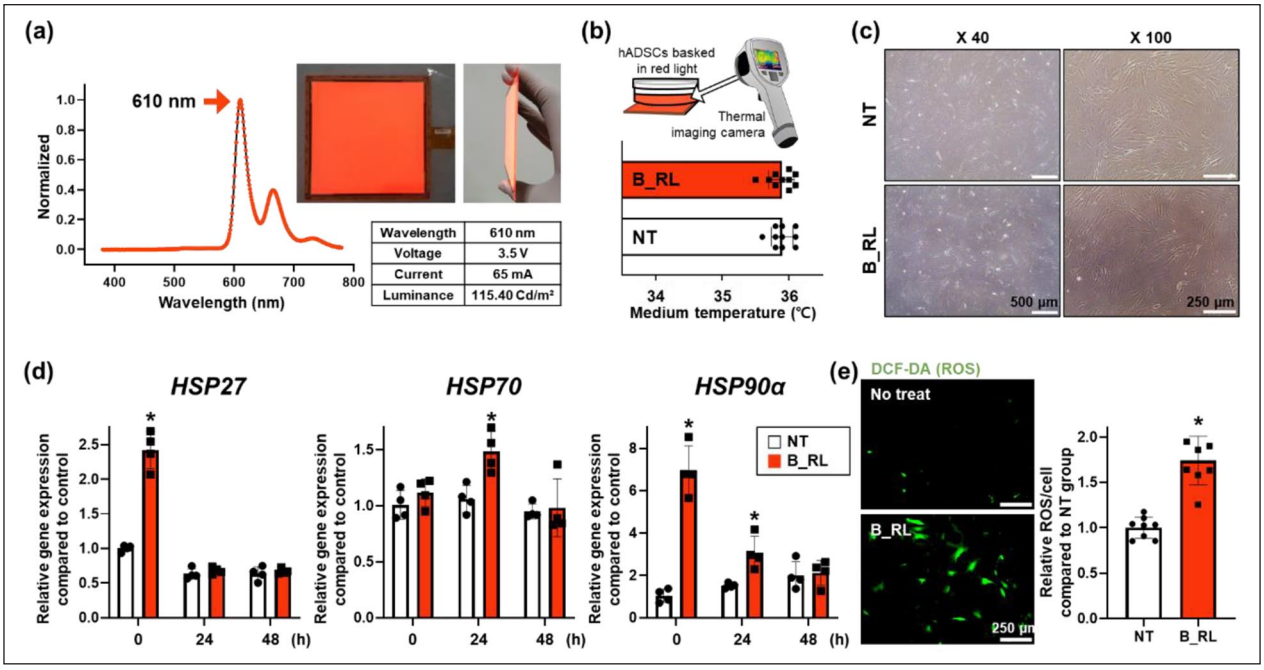

Figure 2. Characteristics of the red organic light-emitting diode (OLED) and the effect of heat emitted from the red OLED on human adipose-derived mesenchymal stem cells (hADSCs). (a) Characteristic and photographs of the red OLED, including wavelength, voltage, current, and luminance. To determine the effect of heat emitted by the red OLED on hADSCs, (b) the temperature of culture medium after B_RL treatment was evaluated using a real-time infrared thermal imaging system. (c) Cell morphology of hADSCs after B_RL treatment. (d) Relative expression of *HSP27*, *HSP70*, and *HSP90α* in hADSCs with B_RL after 0, 24, and 48 h, analyzed with quantitative reverse transcription-PCR (qRT-PCR). No treatment (NT) at 0 h served as the control group (*$p < 0.05$, compared to the NT group at each time point, n = 4). (e) Intracellular ROS staining using DCF-DA (green), and its quantification expressed as percent of fluorescence intensities in the NT group (*$p < 0.05$, compared to that in the NT group, $n = 8$).

USA), which is used as a common dressing material. The wound healing process was observed for up to 14 days after treatment initiation. Wound healing was calculated as the percentage of the initial wound area ([wound area at time]/[initial wound area] × 100%). All samples were collected in an identical manner to allow for an accurate comparison of wound healing in the different groups. Entire tissues from the dorsal wound area were retrieved for analysis to compare the wound healing process in each group.

Histology and immunohistochemistry

Wound tissues from the athymic mice were subjected to various histological examinations. Skin tissue samples were embedded in the optimal cutting temperature compound (O.C.T. compound, Tissue-Plus®; Scigen, Gardena, CA, USA), frozen, and cut into 10 μm sections at −23°C. Overall tissue regeneration was evaluated with hematoxylin and eosin (H&E) and Sirius Red staining and observed under a light microscope (CKX53, Olympus). Sections were subjected to immunofluorescence staining using an anti-Laminine antibody, anti-involucrin antibody (BioLegend, San Diego, CA, USA), and a fluorescein isothiocyanate-conjugated secondary antibody (Jackson ImmunoResearch Laboratories, West Grove, PA, USA) to visualize protein expression and wound repair. The sections were counter-stained with DAPI (VECTASHIELD H-1500, Vector) and examined under a fluorescence microscope (Leica).

Statistical analysis

The GraphPad Prism 7 software was used for all statistical analyses. Triplicate data were analyzed using one-way analysis of variance (ANOVA) with Bonferroni test in all experiments. Comparisons between two independent samples were performed using a two-tailed Student's *t*-test. Statistical significance was set at $p < 0.05$. Results are expressed as mean ± standard deviation for all quantitative analyses.

Results

Effects of red OLED on the heat stress in hADSCs

The properties of red OLED used in this study are shown in Figure 2(a). The wavelength and luminance of this light

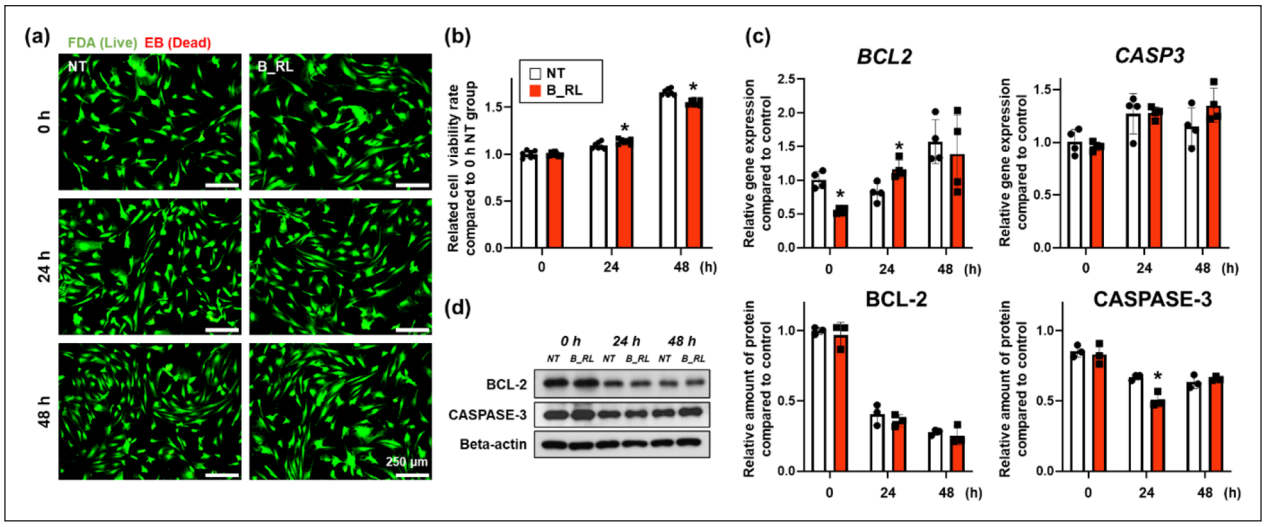

Figure 3. Effects of the B_RL treatment on human adipose-derived mesenchymal stem cells (hADSCs) viability. (a) Viability of the hADSCs basked with red OLED light (B_RL hADSCs) was evaluated with a live/dead assay, which stains live cells green and dead cells red. (b) Viability rate of the B_RL hADSCs was evaluated using the CCK-8 assay (*$p < 0.05$, compared to that in the NT group at each time point). To analyze the relative expression of CASPASE-3 and BCL-2 0, 24, 48 h after B_RL, hADSCs were evaluated with (c) qRT-PCR and (d) western blot analysis. NT at 0 h served as the control group (*$p < 0.05$, compared to that in the NT group at each time point, (c) $n = 4$ and (d) $n = 3$).

source were 610 nm and 115.40 Cd/m^2, respectively. The temperature of the culture medium did not increase when the cells were exposed to B_RL for 24 h (Figure 2(b)). In addition, there was no difference in cell morphology between the NT group and B_RL group (Figure 2(c)). We investigated whether B_RL treatment affects the expression of HSP-family genes related to cellular stress. The expression of *HSP27* and *HSP90α* in hADSCs increased immediately after the B_RL treatment compared to that in the NT group (Figure 2(d)). However, the expression of *HSP27* did not differ from that in the NT group at 24 and 48 h after treatment. The expression of *HSP90α*, which is involved in anti-apoptosis and a prevention of cellular changes,[41] was upregulated up to 24 h. On the other hand, the expression of *HSP70*, induced by stress,[42] increased only 24 h after treatment. Furthermore, immediately after treatment, higher intracellular levels of ROS were detected in the B_RL group than in the NT group (Figure 2(e)). The concentration of intracellular ROS increased approximately 2 times compared to that in the NT group. The expression of the HSP family can be increased to protect cells from oxidative stress such as ROS.[43–46] According to previous studies, oxidative stress applied to cells increases the expression of heat shock factor 1 (HSF1).[43] Increased HSF1 protects cells from oxidative stress by accumulating HSP27, 70, and 90α mRNA in the cells.[43,44] Additionally, it is known that activation of p38MAPKinase and JAK/STAT pathway induce by oxidation stress can upregulate the expression of HSP27 and HSP70 in cells respectively.[45,46] Therefore, the changes in the expression of HSP genes were attributed to the intracellular oxidative stress due to light stimulation rather than heat-induced stress.

Effects of red OLED on the viability of hADSCs

The B_RL treatment did not exhibit cytotoxic effects on hADSCs after 48 h (Figure 3(a)); this treatment slightly increased and then reduced the cellular viability 24 and 48 h after treatment, respectively (Figure 3(b)). Subsequently, the expression of the B-cell lymphoma-2 (BCL-2) and CASPASE-3 was confirmed (Figure 3(c) and (d)). Expression of the *BCL2*, related to anti-apoptosis, showed a tendency to decrease at 0 h but increased 24 h after treatment, and there was no difference between the two groups after 48 h. The B_RL treatment did not alter the expression of the *CASP3*, which is related to apoptosis (Figure 3(c)). On the other hand, there was no difference in the expression of BCL-2 at the protein level between the two groups (Figure 3(d)). In contrast, the expression of CASPASE-3 protein in the B_RL group was slightly decreased 24 h after treatment compared to that in the NT group (Figure 3(d)). Together, our data demonstrate that the B_RL treatment did not affect the viability of hADSCs.

Improvements in the stemness and adhesion of hADSCs using red OLED

The expression of proteins associated with stemness was confirmed using western blotting (Figure 4(a)). Kruppel-like factor 4 (KLF4), sex determining region Y-box 2

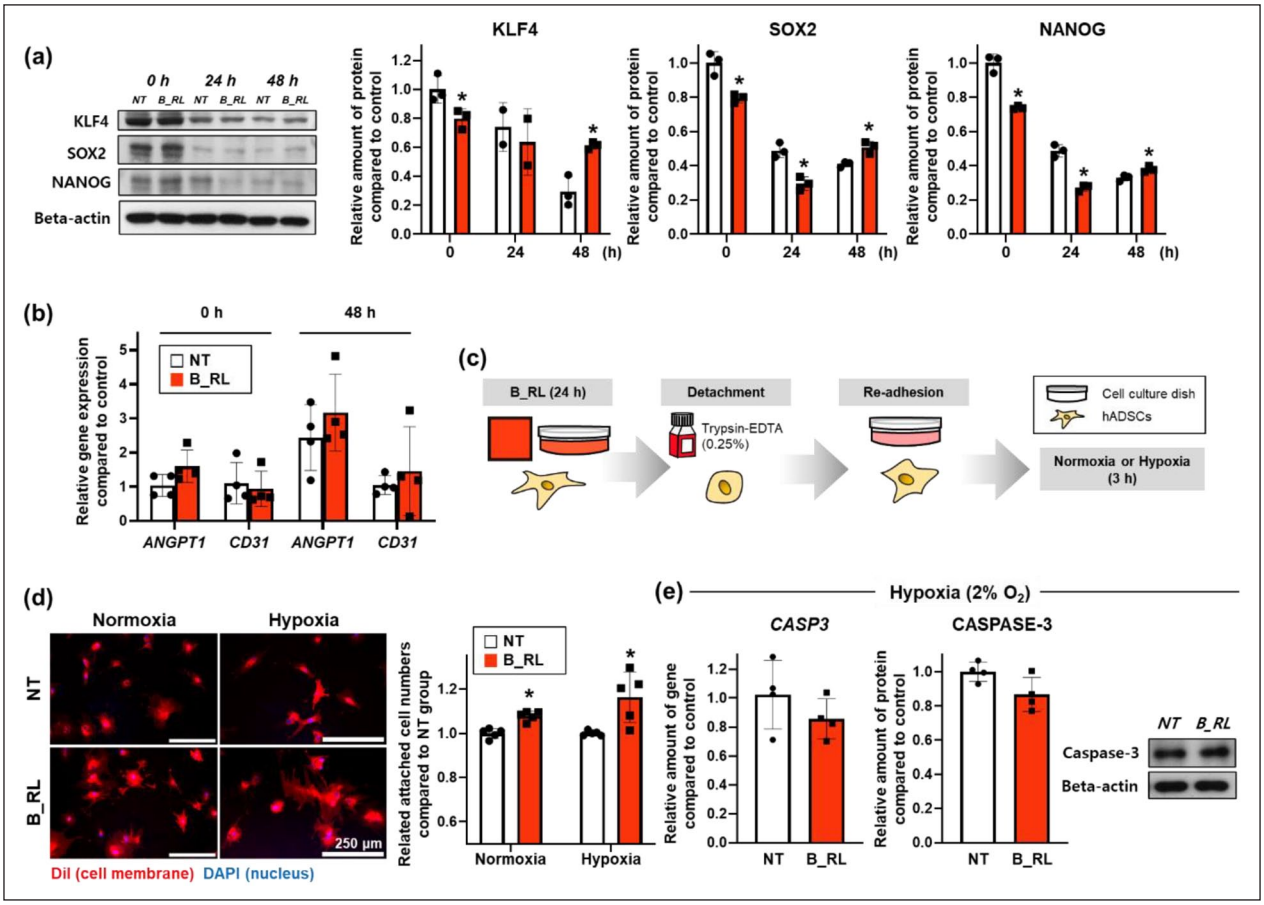

Figure 4. Enhanced stemness and cell adhesion ability of the human adipose-derived mesenchymal stem cells (hADSCs) treated with B_RL. (a) The expression of stemness-related factors (KLF4, SOX2, and NANOG) in hADSCs basked with red OLED light (B_RL hADSCs) after 0, 24, and 48 h was analyzed using western blotting. NT at 0 h served as the control group (*$p < 0.05$, compared to that in the NT group at each time point, $n = 3$). (b) Expression of endothelial differentiation-related genes (*ANGPT1* and *CD31*) in the B_RL hADSCs after 0 and 48 h was analyzed with qRT-PCR. NT at 0 h served as the control group. (c) Cell adhesion was conducted 3 h after the cell re-attachment under normoxic or hypoxic environment to investigate the improvement of adhesion ability of hADSCs following B_RL. (d) Cell adhesion ability was also analyzed using cell membrane staining (DiI: red, DAPI: blue) and the CCK-8 assay (*$p < 0.05$, compared to that in the NT group, $n = 5$). (e) Relative expression of CASPASE-3 in hADSCs was evaluated using qRT-PCR and western blot analysis (3 h after cell re-attachment under hypoxic environment).

(SOX2), and NANOG expression decreased after 0 h, and SOX2 and NANOG expression decreased after 24 h in the B_RL group compared to that in the NT group. However, the expression of these proteins was enhanced in the B_RL group after 48 h compared to that in the NT group. At 0 and 48 h after treatment, there were no differences in the gene expression of angiopoietin-1 (*ANGPT-1*) and *CD31* between the two groups (Figure 4(b)). Both factors are associated with vascular development and angiogenesis, which promotes endothelial differentiation.[47,48] It was found that the B_RL treatment enhanced the stemness of hADSCs, but did not affect endothelial differentiation in vitro. Next, for the re-adhesion test, the hADSCs treated with B_RL for 24 h were detached using trypsin-EDTA and immediately reseeded under normoxic or hypoxic conditions (Figure 4(c)). After 3 h of re-adhesion, the cytoplasm of the B_RL group was wider, and the number of adhered cells had increased compared to that in the NT group (Figure 4(d)). At 3 h after the re-adhesion, there were no differences in the gene expression of *CASP3* between the two groups under normoxia conditions (Supplemental Figure S1). On the other hand, as shown in Figure 4(e), the gene and protein expression of CASPASE-3 slightly decreased in the B_RL group under hypoxic conditions.

Enhanced cellular migration and angiogenesis ability of hADSCs using red OLED

The recovered area after the initial scratch increased significantly in the B_RL groups after 24 and 48 h compared to that in the NT group (Figure 5(a)). The expressions of *CXCL12* and *MMP2*, which are related to cell migration, increased in the B_RL group after 48 h compared to that in

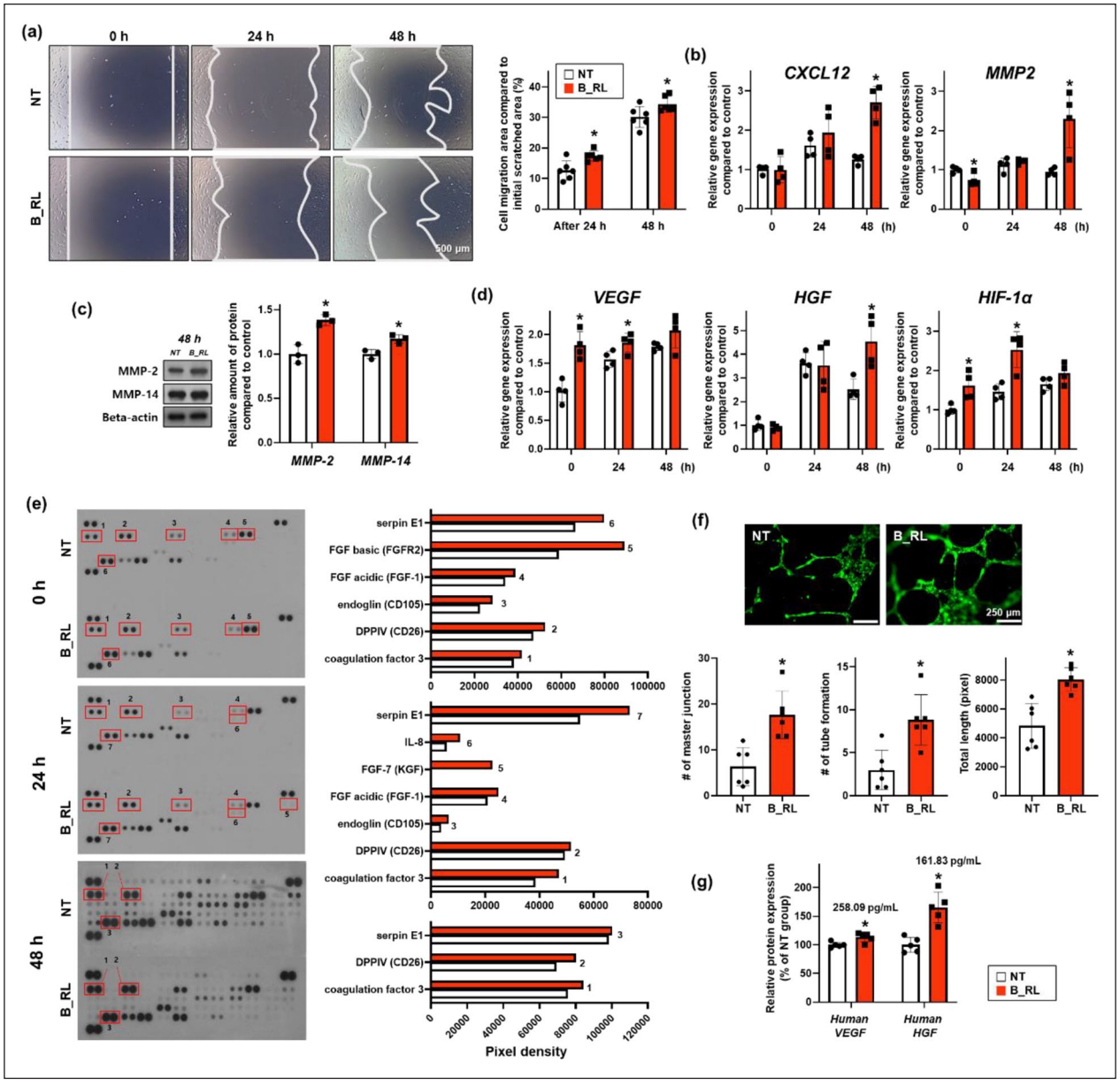

Figure 5. Enhanced cell migration capacity and angiogenic paracrine factors expression in the hADSCs basked with the red OLED light (B_RL hADSCs). (a) Scratch wound coverage assay results showing cell migration capacity. Representative optical images after 0, 24, and 48 h, with quantification (*$p < .05$, compared to that in the NT group, $n = 6$; Scale bar indicates 500 μm). (b) Expression of cell migration-related genes (*CXCL12* and *MMP2*) in B_RL hADSCs after 0, 24, and 48 h, analyzed with qRT-PCR. NT at 0 h served as the control group (*$p < 0.05$, compared to that in the nt group at each time point, $n = 4$). (c) Expression of cell migration-related proteins (MMP-2 and MMP-4) in B_RL hADSCs after 48 h, analyzed with western blotting. NT at 0 h served as the control group (*$p < 0.05$, compared to NT group at each time point, $n = 3$). (d) Expression of angiogenesis-related genes (*VEGF*, *HGF*, and *HIF-1*α) in B_RL hADSCs after 0, 24, and 48 h, analyzed with qRT-PCR. NT at 0 h served as the control group (*$p < 0.05$, compared to that in the NT group at each time point, $n = 4$). (e) Expression of angiogenesis-related proteins in B_RL hADSCs after 0, 24, and 48 h, analyzed with human angiogenesis array. Representative image of the human angiogenesis array data and comparison of quantitative difference. Angiogenic capacity based on paracrine factor secretion in B_RL hADSCs was evaluated by (f) HUVEC tube formation and (g) ELISA (VEGF, HGF). Conditioned medium was collected from B_RL hADSCs after 0 and 48 h. (f) HUVEC tube formation assay after incubating HUVECs (green) with conditioned medium retrieved from the B_RL hADSCs (0 h) with quantification (*$p < 0.05$, compared to that in the NT group, $n = 6$). (g) Angiogenesis-related factors secreted in the conditioned medium from B_RL hADSCs (48 h), evaluated with ELISA (*$p < 0.05$, compared to that in the NT group, $n = 5$).

the NT group (Figure 5(b)). In addition, the expression of matrix metalloproteinase (MMP-2 and MMP-14), which are related to cell migration, increased in the B_RL group after 48 h compared with that in the NT group (Figure 5(c)). These results indicated that the B_RL treatment not only improved the migration ability of hADSCs but also

augmented cell recruitment, which is essential for the treatment of wounds in vivo. Subsequently, it was confirmed that the expression of vascular endothelial growth factor (*VEGF*), hepatocyte growth factor (*HGF*), and hypoxia-inducible factor 1-alpha (*HIF-1α*), associated with angiogenesis, increased in the B_RL group at some time points (Figure 5(d)).[49] The cell lysates were analyzed using an angiogenesis antibody array (Figure 5(e)). The angiogenesis-related factors that increased at all time points were coagulation factor 3, DPPIV, and serpin E1. Coagulation factor 3 (TF) is a factor that improves angiogenesis. DDPIV, also known as CD26, not only enhances angiogenesis, but also plays an important role in cellular adhesion between ECM and cells.[50,51] Serpin E1 promotes angiogenesis and induces cell migration as an essential factor for wound repair.[52] Immediately after the cells were basked in red light, the CD105, FGF acidic, and FGF basic factors were further improved. In particular, FGF basic, associated with scarless wound healing, increased in the B_RL group. This factor regulates the synthesis and deposition of various ECMs.[53] Twenty-four hours after treatment, CD105, FGF acidic, FGF-7, and IL-8 were further increased in the B_RL group. In particular, FGF-7 was identified only in the B_RL group, which plays an important role in re-epithelialization by stimulating the proliferation and migration of keratinocytes. FGF-7 is also known to play an important role in the final stages of neovascularization.[53] The angiogenesis ability was confirmed in vitro through tube formation experiments using the conditioned medium from B_RL treated hADSCs (Figure 5(f)). It was confirmed that the angiogenesis ability of HUVECs treated with conditioned medium from the B_RL group was enhanced in all aspects of the HUVEC's master junction, tube formation, and total length compared to those of the NT group. Subsequently, the secretion of VEGF and HGF from the B_RL-treated hADSCs was confirmed using ELISA (Figure 5(g)). At 48 h, the secretion of both VEGF and HGF increased in the B_RL group compared to that in the NT group.

Accelerated wound healing of red OLED-treated hADSCs

The therapeutic efficacy of B_RL-treated hADSCs was evaluated using a mouse wound healing model. Since wound regeneration is a complex process, it is important to select an appropriate animal model considering the specifics of wounds (e.g. size, location, depth).[54] To confirm the beneficial therapeutic effect on large wounds, following the induction of 2.0 cm × 2.0 cm square-shaped full-thickness skin defects, and then the mice were treated with hADSCs transplantation and covered with Tegaderm™. Based on results of the in vitro tests, we expected that the therapeutic effects of B_RL-treated hADSCs would be greater than those of the untreated hADSCs (Figure 6(a)). We divided the mice into the following three groups: Tegaderm™ (T), 0.5×10^6 hADSCs per mouse with Tegaderm™ (Cell + T (C@T)), and 0.5×10^6 B_RL-treated hADSCs per mouse with Tegaderm™ (B_RL Cell + T (B_RL C@T)). Representative photographs of the mice at 0, 7, and 14 days after treatment are shown in Figure 6(b). Skin wound areas were measured on days 0 and 14. Wound closure is represented as a percentage of the original wound area. The B_RL C@T group exhibited a significantly increased therapeutic effect than the other groups. It was confirmed via IHC staining and western blot assay that the expression of laminin and involucrin in the skin tissue was increased in the B_RL C@T group compared to that in the other groups (Figure 6(c)). Laminin is an ECM component that constitutes the basement membrane of the skin,[55–57] and involucrin is an ECM component that plays an important role in the barrier function of the skin.[58–60] Next, using H&E and Sirius Red staining, it was confirmed that the structure of skin tissue from the B_RL C@T group was similar to that of normal skin (Figure 6(d)). In addition, amount of Col I protein in the skin tissue was the highest in the B_RL C@T group compared to that in the other groups (Figure 6(e)). Col I is a major structural protein that constitutes ECM and is known to promote the wound healing process.[61] Subsequently, it was confirmed that the gene expression of *Progranulin* and transforming growth factor beta 1 (*Tgf-β1*) increased dramatically in the B_RL C@T group (Figure 6(f)). Progranulin and Tgf- β1 are factors that play important roles in the overall process of wound healing and are known to stimulate various cells at the wound site.[62–64] Therefore, the increase in the gene expression of both factors indicates that the wound healing process actively progressed in the skin wound. Overall, our data indicate that the B_RL C@T group can accelerate the wound healing process and improve structural restoration of skin defects, which is likely attributed to an increased adaptation ability under hypoxic conditions (Figure 4) and enhanced angiogenesis ability (Figure 5) of hADSCs by the B_RL treatment.

Discussion

In this study, using a different light source from that used in previous studies, we optimized the parameters of OLED-based PBM for stem cells and focused on enhancing the stem cell treatment efficiency. After the irradiation of hADSCs with OLED light, cell adhesion, migration ability, and stemness improved without the introduction of external genes or drugs while maintaining cell viability. When the B_RL hADSCs were transplanted into an in vivo mouse wound healing model, angiogenesis was stimulated by the elevated paracrine effects of the angiogenic factors. In addition, we confirmed that wound closure was accelerated in the mice transplanted with B_RL hADSCs than the

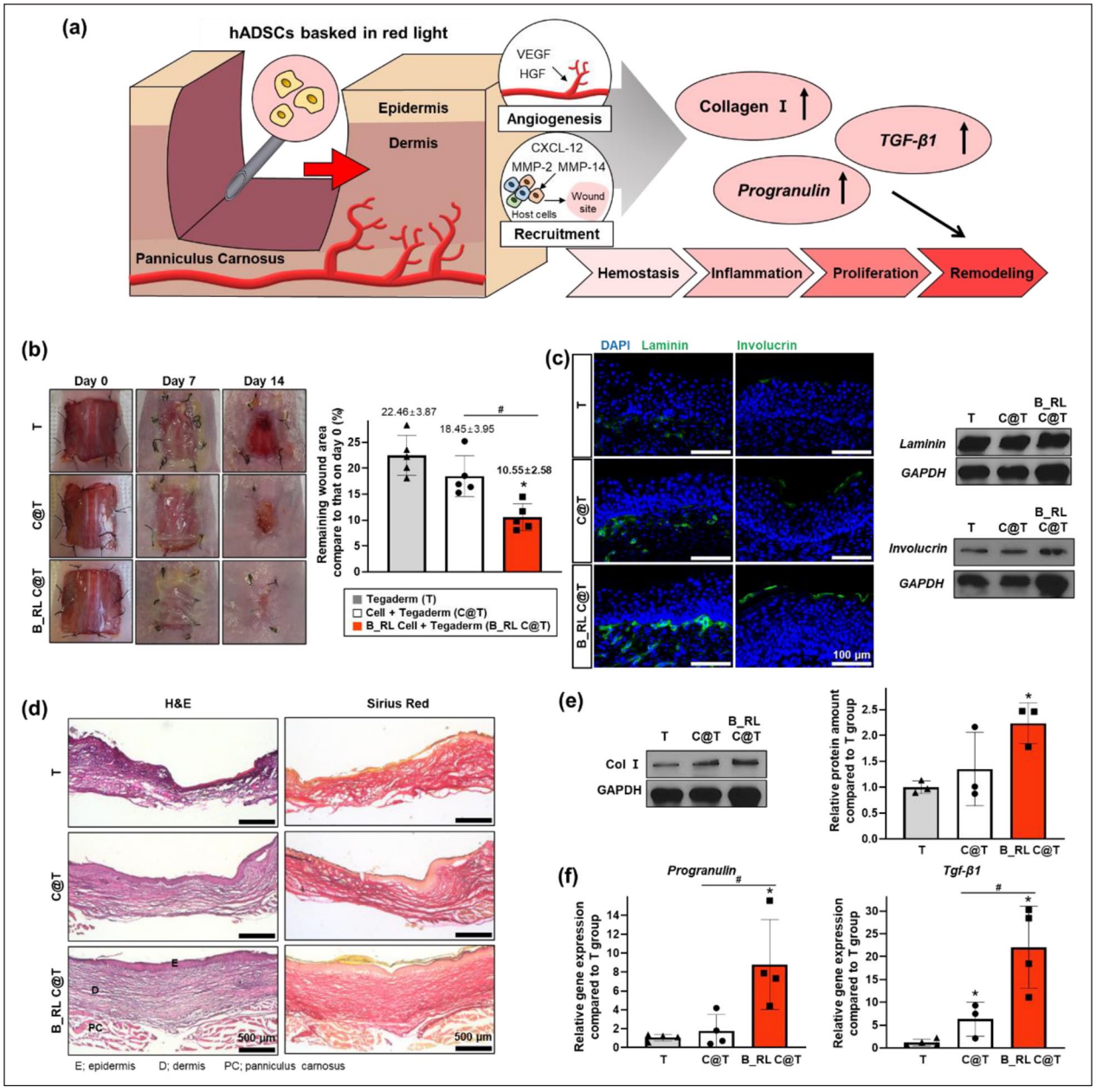

Figure 6. In vivo wound closure induced by red OLED light-basked hADSCs. (a) Schematic of the mouse skin wound healing model using hADSCs basked in red light. (b) Representative images of the wound at 0, 7, and 14 days after various treatments. Quantification of wound closure at day 14 after treatments for all groups (*$p < 0.05$, compared with that in the t group; #$p < 0.05$, compared with each group, $n = 5$). (c) Immunohistochemistry for laminin (green) or involucrin (green) with DAPI (blue) staining in skin wound at 14 days after treatment (left). Relative expression of laminin and involucrin in the wound region at 14 days after treatment (right, western blot analysis). (d) Representative H&E and Sirius Red stained images of the tissue sections from the skin wound models at 14 days after treatment. Relative expression of (e) Col I, (f) *Progranulin*, and *Tgf*-β in the wound region at 14 days after treatment. (*$p < 0.05$, compared with that in the t group; #$p < 0.05$, compared with each group, (e) $n = 3$ and (f) $n = 4$).

mice treated with conventional methods (Figure 1). Point light source-based lasers and LEDs, originally used as PBM materials, have too many limitations, such as poor irradiation uniformity and difficult applicability, to be used as a commercial light source.[3,6,11,65,66] Moreover, there are potential concerns, such as the bulkiness of complex irradiation systems and heat damage to cells.[66–68] OLEDs are surface light sources that do not require a heat sink, and it is possible to uniformly expose a large area.[24,66] Thus, we suggest a new strategy to increase stem cell efficiency by applying OLEDs to PBM, which can overcome the disadvantages of existing PBM materials (LED, laser).

In general, the depth of penetration into the skin varies depending on the wavelength. Blue (400–470 nm) and green (470–550 nm) light can be used to treat skin from the epidermis to the dermis, and wavelength of 600–1000 nm penetrates further. The range from visible red to near-infrared light (600–1000 nm) is mostly used to heal hypodermis tissue during wound healing.[2–4] Therefore, we used an OLED light source belonging to the red wavelength, for skin wound treatment (Figure 2(a)). Temperature of the medium in which the hADSCs were cultured, was measured to determine whether the hADSCs were influenced by heat. Resultantly, no difference was observed between the experimental groups (Figure 2(b)). According to previous studies, the activity of CCO, complex IV constituting the mitochondrial electron transport chain, is increased by absorption of light energy, and NO is photodissociated from CCO, which leads to the enhancement of NO concentration. As a result, an electrochemical proton gradient is generated as electron transport occurs in the inner mitochondrial membrane, and the synthesis of ATP is increased by a proton gradient with ROS levels increment.[2,4,6] Interestingly, we found that intracellular ROS levels (1.74-fold) were enhanced by OLED red light (Figure 2(e)), but the light did not affect NO or ATP production in hADSCs as reported previously (Supplemental Figure S2).[2,4,6] Although the accumulation of ROS negatively affects cells, several studies have shown that a mild concentration of ROS acts as a secondary messenger or performs a beneficial function in stabilizing the expression of HIF-1α.[69–71] Furthermore, the upregulated HSP expression appears to be affected by ROS rather than by temperature (Figure 2(d)). HSP is well known as a protein that plays a cytoprotective role in response to various environmental stresses or pathophysiological states, including ROS.[46,71–73] The major molecular roles of the HSP chaperone are protein folding, refolding/denaturation of misfolded proteins, and assembling/disassembling of proteins.[71,72] The HSP family is also involved in the apoptosis-related pathway and, in particular, HSP27 controls inflammation. Additionally, HSP70 plays an important role in skin rejuvenation by supporting the synthesis, folding, and transport of collagen, and HSP90 increases the wound healing process by promoting the migration of cells that are present near the wound site.[6,74,75] It has been demonstrated that the expression of HSP27, 70, and 90 is promoted by PBM,[74,75] and the activated expression of HSP27, 70, and 90 would have a positive effect on wound healing and inflammation.

We confirmed that the hADSCs survived without cell death immediately after OLED red light irradiation (Figure 3(a) and (b)) and demonstrated that there was no toxicity of PBM using OLEDs by maintaining cellular viability. In this regard, the B_RL hADSCs showed similar expression of the genes and proteins related to apoptosis (CASPASE-3) and anti-apoptosis (BCL-2) as that in the conventional hADSCs that had not been irradiated OLEDs until 48 h after irradiation (Figure 3(c) and (d)). In other words, we verified that the new strategy using OLEDs is a way to overcome the problems of previous PBM while maintaining safety. Most studies conducted using irradiating LEDs or lasers on stem cells are controversial; they either revealed that the differentiation of stem cells is induced,[13,14,76–78] or that there is no change in differentiation[79,80] after light irradiation. However, the PBM of OLED irradiation did not induce differentiation in a specific direction and, instead, the stemness of hADSCs themselves increased. KLF4, SOX2, and Nanog, which are known transcription factors, inhibit the expression of differentiation-associated genes of stem cells and are highly expressed in undifferentiated stem cells. Thus, they have been identified as stemness markers in stem cell studies.[1,81–83] Hence, we determined the expression of KLF4, SOX2, and Nanog, and found that decreased until 24 h after the irradiation of hADSCs with OLEDs. However, at 48 h after irradiation, levels of the stemness marker increased compared to those in the conventional hADSCs (Figure 4(a)). An increase in the expression of stemness-related factors means that the multilineage potential of hADSCs is increased. Since the underlying properties of hADSCs such as self-renewal and differentiation ability, have been improved by OLED-based PBM, their efficiency as a source of stem cell therapy has been enhanced.[65,67–69,79,81–83] Moreover, when OLED light is applied to wound treatment, angiogenesis and wound healing can be promoted by stimulated secretion of various cytokines and growth factors as much as the efficiency of stem cells improves.[14,35,76]

To verify the effectiveness of OLED-based PBM, we examined the cell adhesion and migration ability, among various biological processes. Adhesion ability was assessed so as to mimic the hypoxic environment experienced after hADSCs cultured *in vitro* were transplanted to the wound site of an in vivo mouse model. After OLED light irradiation, hADSCs were dissociated and re-adhered, and then cultured under normoxic/hypoxic conditions for 3 h (Figure 4(c)). As a result, the experimental group showed increased adhesion ability not only under normoxic conditions compared to the control group but also under hypoxic conditions (Figure 4(d)). Through the expression of CASPASE-3, it was confirmed that cell viability was maintained under hypoxic conditions (Figure 4(e)). We concluded that when hADSCs were transplanted into the wound sites, the B_RL hADSCs had increased adhesion ability compared to conventional hADSCs and the viability was also maintained. Based on the study results that showed PBM irradiation increases cell migration efficacy, a scratch assay was conducted and migration-related factors were identified.[1,4,6,84] In order for cell migration to occur, a process of decomposing matrix barriers using specific enzymes is required. In this process, MMPs play an important role in removing extracellular

matrix (ECM) and damaged proteins at the inflammatory stage.[85,86] The factors we identified are known as gelatinase for MMP2, membrane-type metalloproteinase for MMP14, and macrophage metalloelastase for MMP12.[85–87] At 48 h after light exposure, the migration ability of B_RL hADSCs significantly increased, which contributed to facilitating wound repair (Figure 5(a)–(c)). Angiogenesis is an essential physiological process in wound healing. There are reports that the enhancement pattern of angiogenic properties by PBM is remarkably stimulated not only in in vivo models but also in the in vitro experiments.[1,4,6,22] Thus, we hypothesized that the expression of angiogenic factors in hADSCs would increase and wound healing would be accelerated by OLED-based PBM, and confirmed the expression of angiogenesis-related factors, which are the most representative markers (VEGF and HGF) in the in vitro experiments. Immediately after red-light irradiation for 48 h, the gene/protein expression of VEGF and HGF was higher than that of the hADSCs that were not irradiated with OLEDs (Figure 5(d) and (g)). Upon screening for various types of angiogenesis-related factors, specific markers showed a steadily increasing trend, and the most factors were stimulated at 24 h after OLED exposure (Figure 5(e)). Interestingly, the expression of HIF-1α, which is a known transcription factor, also improved, as shown in previous studies (Figure 5(d)).[6,88] As HIF-1α plays an essential role in the molecular regulation of angiogenesis,[14,88,89] the upregulated angiogenic paracrine effect seems to be due to the activated HIF-1α. Moreover, increased intracellular ROS levels caused by PBM are associated with HIF-1α as well as HSP, which could have activated HIF-1α.[90–92] Studies have also reported that the HIF-1α is regulated by activation of the PI3K and MAPK/ERK pathways, and receptor tyrosine kinases (RTKs), cell surface receptors, act as ligands for PI3K and MAPK/ERK signaling.[1,20,21] For angiogenesis, not only paracrine factors, but also the promotion of new capillary formation and blood flow is required. Previous studies reported that tube formation in HUVECs is stimulated by PBM,[20,88] therefore, we analyzed whether OLED-based PBM also affects the tube formation in HUVECs. Tube formation of HUVECs was promoted (Figure 5(f)), which had a positive effect on wound healing with angiogenesis-related factors.

Finally, the hADSCs with improved efficiency due to OLED-based PBM were injected into the in vivo mouse wound healing model to confirm the wound repair effect (Figure 6(a)). After hADSC transplantation, mice were observed for up to 14 days, and the wound area of the group injected with B_RL hADSC decreased faster than that of the group injected with hADSCs that were not irradiated, resulting in accelerated healing (Figure 6(b)). Additionally, to determine the treatment progress of the damaged skin layer, laminin and involucrin were analyzed using immunohistochemistry and protein expression, following extraction from mouse wound skin. Laminin is an essential protein constituting the skin basement membrane, and it contributes to the structure of ECM by interacting with type IV collagen.[55–57] Furthermore, involucrin is a marker expressed in the stratum corneum (cornified layer) of the skin and is known to form the cornified envelope membrane of the corneocyte by cross-linking with other structural proteins.[58–60] The expression of laminin and involucrin was promoted compared to that in the group transplanted with hADSCs that did not receive OLED stimulation (Figure 6(c)) indicating that the stimulating effect of OLED-based PBM not only accelerates wound closure but also effectively maintains the skin layer itself. In particular, the dermis in the skin layer was thicker than that in the conventional groups. The collagen that composes most of the dermis was confirmed through staining and protein expression, and it was also found to be significantly stimulated (Figure 6(d) and (e)). When tissue is damaged, anti-inflammatory cytokines are secreted by macrophages and neutrophils to suppress inflammation. Tgf-ß, a representative cytokine, has been reported to inhibit immune response and be involved in wound healing and angiogenesis.[93–95] Moreover, Tgf-ß stimulates endothelial cell migration and ECM synthesis by the production of collagen.[29,32,64] Another mediator protein, Progranulin is known to have an activity that regulates inflammation.[96] Therefore, we investigated the gene expression of Tgf-ß and Progranulin as anti-inflammatory markers (Figure 6(f)). It was demonstrated that the inflammatory response of the damaged wound site was regulated by the inhibitory effect of B_RL hADSCs through the highly enhanced expression of Tgf-ß and Progranulin. The expression of CD31 in B_RL hADSCs group was significantly upregulated in comparison with the other group (Supplemental Figure S3). In conclusion, hADSCs whose efficiency was enhanced by stimulation with OLED-based PBM, demonstrated their strength as a source of stem cell therapy through their effect in the wound healing model.

Conclusions

In this study, hADSCs were exposed to red light using a different light source from the materials used in previous PBM studies, and the B_RL-treated hADSCs maintained cell viability without heat damage. The stemness of B_RL hADSCs was improved, and cell adhesion, migration capability, and secretion of angiogenic factors were also stimulated, thereby enhancing the therapeutic efficiency of hADSCs. Furthermore, transplantation of the B_RL hADSCs into the wound site proved to be a more effective stem cell therapy than the conventional treatment of hADSCs injection without OLED irradiation. PBM using OLEDs influences hADSCs to have an increased angiogenic effect and wound closing effect, and it could also be suggested as

an alternative material to replace PBM materials. OLEDs are material that can emit light without heat, can be produced in a thin film or bendable form, and can uniformly emit light over a large area, surpassing the limitations of existing PBM. Moreover, a simple setup is possible and can be easily applied to currently used PBM-based equipment.[50] We proposed this strategy to promote the efficiency of stem cells via OLED-based PBM. This approach has the advantage that it can be applied to various clinical stem cell therapies and in consequence, photodynamic stem cell therapy using OLEDs may become a new paradigm in the cell therapy field of tissue regenerative medicine.

Acknowledgements

Yu-Jin Kim and Hye Ran Jeon contributed equally to this work. No other persons besides the authors have made substantial contributions to this manuscript.

Authors' contributions

The authors declare that the data supporting the findings of this study are available within the paper and its supplementary information. Conceptualization: YJK, HRJ, DIK, and SHB; Methodology: YJK, HRJ, SWK, YHK, GBI, and JI; Formal analysis: YJK, HRJ, DIK, and SHB; Investigation: YJK, HRJ, SWK, YHK, GBI, and JI; Writing—original Draft: YJK, HRJ, DIK, and SHB; Writing—review and editing: SHU, SMC, JRL, HYK, YKJ, DIK, and SHB; Visualization: YJK and HRJ; Supervision: SMC, DIK, and SHB; Funding acquisition: SHU, YKJ, DIK, and SHB. All authors read and approved the final manuscript.

Availability of data and materials

The datasets used and/or analyzed during the current study are available from the corresponding author on reasonable request.

Declaration of conflicting interests

The author(s) declared no potential conflicts of interest with respect to the research, authorship, and/or publication of this article.

Ethics approval

All animal treatments and experimental procedures were approved by the Institutional Animal Care and Use Committee of SKKU (SKKUIACUC2020-06-11-1).

Funding

The author(s) disclosed receipt of the following financial support for the research, authorship, and/or publication of this article: This work was supported by the National Research Foundation of Korea (NRF) and the Ministry of Science and ICT (MSIT) (2019R1C1C1007384, 2018M3A9E2023255, 2020M2D9A3094171, 2021R1A4A1032782). This research was also supported by the Korea Medical Device Development Fund graft funded by the Korea government (the Ministry of Science and ICT, the Ministry of Trade, Industry and Energy, the Ministry of Health & Welfare, and the Ministry of Food and Drug Safety, Republic of Korea, Project Number: 202011B31). This work is partially funded by a grant from the Basic Science Research Program through the National Research Foundation of Korea funded by the Ministry of Science, ICT, and Future Planning (Grant no. 2019R1A2C2002390)

ORCID iD

Suk Ho Bhang https://orcid.org/0000-0003-3002-0590

Supplemental material

Supplemental material for this article is available online.

References

1. Ahrabi B, Rezaei Tavirani M, Khoramgah MS, et al. The effect of photobiomodulation therapy on the differentiation, proliferation, and migration of the mesenchymal stem cell: a review. *J Laser Med Sci* 2019; 10: S96–S103.
2. Avci P, Gupta A, Sadasivam M, et al. Low-level laser (light) therapy (LLLT) in skin: stimulating, healing, restoring. *Semin Cutan Med Surg* 2013; 32(1): 41–52.
3. Barolet D. Light-emitting diodes (LEDs) in dermatology. *Semin Cutan Med Surg* 2008; 27(4): 227–238.
4. Dompe C, Moncrieff L, Matys J, et al. Photobiomodulation—underlying mechanism and clinical applications. *J Clin Med* 2020; 9: 1724.
5. DeLand MM, Weiss RA, McDaniel DH, et al. Treatment of radiation-induced dermatitis with light-emitting diode (LED) photomodulation. *Lasers Surg Med* 2007; 39: 164–168.
6. de Freitas LF and Hamblin MR. Proposed mechanisms of photobiomodulation or low-level light therapy. *IEEE J Sel Top Quantum Electron* 2016; 22: 348–364.
7. Oliveira CG, Freitas MF, de Sousa MVP, et al. Photobiomodulation reduces nociception and edema in a CFA-induced muscle pain model: effects of LLLT and LEDT. *Photochem Photobiol Sci* 2020; 19: 1392–1401.
8. Stergioulas A. Low-level laser treatment can reduce edema in second degree ankle sprains. *J Clin Laser Med Surg* 2004; 22: 125–128.
9. Alexiades M. Laser and light-based treatments of acne and acne scarring. *Clin Dermatol* 2017; 35: 183–189.
10. Papageorgiou P, Katsambas A and Chu A. Phototherapy with blue (415 nm) and red (660 nm) light in the treatment of acne vulgaris. *Br J Dermatol* 2000; 142: 973–978.
11. Caetano KS, Frade MA, Minatel DG, et al. Phototherapy improves healing of chronic venous ulcers. *Photomed Laser Surg* 2009; 27: 111–118.
12. Minatel DG, Frade MAC, França SC, et al. Phototherapy promotes healing of chronic diabetic leg ulcers that failed to respond to other therapies. *Lasers Surg Med* 2009; 41: 433–441.
13. Chen H, Wu H, Yin H, et al. Effect of photobiomodulation on neural differentiation of human umbilical cord mesenchymal stem cells. *Lasers Med Sci* 2019; 34: 667–675.
14. Park I-S, Chung P-S and Ahn JC. Enhancement of ischemic wound healing by spheroid grafting of human adipose-derived stem cells treated with low-level light irradiation. *PLoS One* 2015; 10: e0122776.
15. Jeon Y, Choi H-R, Kwon JH, et al. 22-4: wearable photobiomodulation patch using attachable flexible organic light-emitting diodes for human keratinocyte cells. *SID Symp Dig Tech Pap* 2018; 49(1): 279–282.

16. do Valle IB, Prazeres PHDM, Mesquita RA, et al. Photobiomodulation drives pericyte mobilization towards skin regeneration. *Sci Rep* 2020; 10: 19257.
17. Li W, Chen H and Wang C. Effect of light emitting diode irradiation on proliferation of human bone marrow mesenchymal stem cells. *J Med Biol Eng* 2006; 26: 35.
18. Tao C-Y, Lee N, Chang H-C, et al. Evaluation of 660 nm LED light irradiation on the strategies for treating experimental periodontal intrabony defects. *Lasers Med Sci* 2016; 31: 1113–1121.
19. Dang Y, Liu B, Liu L, et al. The 800-nm diode laser irradiation induces skin collagen synthesis by stimulating TGF-β/Smad signaling pathway. *Lasers Med Sci* 2011; 26: 837–843.
20. Chen CH, Hung HS and Hsu SH. Low-energy laser irradiation increases endothelial cell proliferation, migration, and eNOS gene expression possibly via PI3K signal pathway. *Lasers Surg Med* 2008; 40: 46–54.
21. Shefer G, Oron U, Irintchev A, et al. Skeletal muscle cell activation by low-energy laser irradiation: a role for the MAPK/ERK pathway. *J Cell Physiol* 2001; 187: 73–80.
22. Yin K, Zhu R, Wang S, et al. Low-level laser effect on proliferation, migration, and antiapoptosis of mesenchymal stem cells. *Stem Cells Dev* 2017; 26: 762–775.
23. Jou J-H, Chou K-Y, Yang F-C, et al. A universal, easy-to-apply light-quality index based on natural light spectrum resemblance. *Appl Phys Lett* 2014; 104: 203304.
24. Geffroy B, le Roy P and Prat C. Organic light-emitting diode (OLED) technology: materials, devices and display technologies. *Polym Int* 2006; 55: 572–582.
25. Jeon Y, Choi HR, Lim M, et al. A wearable photobiomodulation patch using a flexible red-wavelength OLED and its in vitro differential cell proliferation effects. *Adv Mater Technol* 2018; 3: 1700391.
26. Wu X, Alberico S, Saidu E, et al. Organic light emitting diode improves diabetic cutaneous wound healing in rats. *Wound Repair Regen* 2015; 23: 104–114.
27. Qi X, Pan W, Tong X, et al. ε-Polylysine-stabilized agarose/polydopamine hydrogel dressings with robust photothermal property for wound healing. *Carbohydr Polym* 2021; 264: 118046.
28. Zeng Q, Qian Y, Huang Y, et al. Polydopamine nanoparticle-dotted food gum hydrogel with excellent antibacterial activity and rapid shape adaptability for accelerated bacteria-infected wound healing. *Bioact Mater* 2021; 6: 2647–2657.
29. Zhao X, Wu H, Guo B, et al. Antibacterial anti-oxidant electroactive injectable hydrogel as self-healing wound dressing with hemostasis and adhesiveness for cutaneous wound healing. *Biomaterials* 2017; 122: 34–47.
30. Yang Y, Zhao X, Yu J, et al. Bioactive skin-mimicking hydrogel band-aids for diabetic wound healing and infectious skin incision treatment. *Bioact Mater* 2021; 6: 3962–3975.
31. Zhao X, Liang Y, Huang Y, et al. Physical double-network hydrogel adhesives with rapid shape adaptability, fast self-healing, antioxidant and NIR/pH stimulus-responsiveness for multidrug-resistant bacterial infection and removable wound dressing. *Adv Funct Mater* 2020; 30: 1910748.
32. Zhao X, Pei D, Yang Y, et al. Green tea derivative driven smart hydrogels with desired functions for chronic diabetic wound treatment. *Adv Funct Mater* 2021; 31: 2009442.
33. Zhang M, Huang Y, Pan W, et al. Polydopamine-incorporated dextran hydrogel drug carrier with tailorable structure for wound healing. *Carbohydr Polym* 2021; 253: 117213.
34. Chen T, Chen Y, Rehman HU, et al. Ultratough, self-healing, and tissue-adhesive hydrogel for wound dressing. *ACS Appl Mater Interfaces* 2018; 10: 33523–33531.
35. Tonnesen MG, Feng X and Clark RAF. Angiogenesis in wound healing. *J Investig Dermatol Symp Proc* 2000; 5: 40–46.
36. Guerra A, Belinha J and Jorge RN. Modelling skin wound healing angiogenesis: a review. *J Theor Biol* 2018; 459: 1–17.
37. Zhang JD, Ruschhaupt M and Biczok R. DdCt method for qRT–PCR data analysis. *Citeseer* 2013. http://www.bioconductor.org/packages/release/bioc/html/ddCt.html
38. Liang C-C, Park AY and Guan J-L. In vitro scratch assay: a convenient and inexpensive method for analysis of cell migration in vitro. *Nat Protoc* 2007; 2: 329–333.
39. Dai T, Kharkwal GB, Tanaka M, et al. Animal models of external traumatic wound infections. *Virulence* 2011; 2: 296–315.
40. Tan MK, Hasan Adli DS, Tumiran MA, et al. The efficacy of Gelam honey dressing towards excisional wound healing. *Evid Based Complement Alternat Med* 2012; 2012: 805932.
41. Arya R, Mallik M and Lakhotia SC. Heat shock genes - integrating cell survival and death. *J Biosci* 2007; 32: 595–610.
42. Parida S, Mishra SR, Mishra C, et al. Impact of heat stress on transcriptional abundance of HSP70 in cardiac cells of goat. *Anim Biotechnol* 2020; 31: 223–228.
43. Nishizawa J, Nakai A, Matsuda K, et al. Reactive oxygen species play an important role in the activation of heat shock factor 1 in ischemic-reperfused heart. *Circulation* 1999; 99: 934–941.
44. Prodromou C. Mechanisms of Hsp90 regulation. *Biochem J* 2016; 473: 2439–2452.
45. Yu AL, Fuchshofer R, Birke M, et al. Oxidative stress and TGF-β2 increase heat shock protein 27 expression in human optic nerve head astrocytes. *Investig Ophthalmol Vis Sci* 2008; 49: 5403–5411.
46. Madamanchi NR, Li S, Patterson C, et al. Reactive oxygen species regulate heat-shock protein 70 via the JAK/STAT pathway. *Arterioscler Thromb Vasc Biol* 2001; 21: 321–326.
47. Joo HJ, Kim H, Park S-W, et al. Angiopoietin-1 promotes endothelial differentiation from embryonic stem cells and induced pluripotent stem cells. *Blood* 2011; 118: 2094–2104.
48. Meng X, Chen M, Su W, et al. The differentiation of mesenchymal stem cells to vascular cells regulated by the HMGB1/RAGE axis: its application in cell therapy for transplant arteriosclerosis. *Stem Cell Res Ther* 2018; 9(1): 85.
49. Kim Y, Kim S, Im G, et al. Area light source-triggered latent angiogenic molecular mechanisms intensify therapeutic efficacy of adult stem cells. *Bioeng Transl Med* 2021; 2021: e10255.

50. Zheng X, Liu J, Li X, et al. Angiogenesis is promoted by exosomal DPP4 derived from 5-fluorouracil-resistant colon cancer cells. *Cancer Lett* 2021; 497: 190–201.
51. Nishida H, Hayashi M, Morimoto C, et al. CD26 is a potential therapeutic target by humanized monoclonal antibody for the treatment of multiple myeloma. *Blood Cancer J* 2018; 8: 99.
52. Simone TM, Higgins CE, Czekay R-P, et al. SERPINE1: a molecular switch in the proliferation-migration dichotomy in wound-"activated" keratinocytes. *Adv Wound Care* 2014; 3: 281–290.
53. Barrientos S, Stojadinovic O, Golinko MS, et al. Growth factors and cytokines in wound healing. *Wound Repair Regen* 2008; 16: 585–601.
54. Rittié L. Cellular mechanisms of skin repair in humans and other mammals. *J Cell Commun Signal* 2016; 10: 103–120.
55. Aumailley M and Smyth N. The role of laminins in basement membrane function. *J Anat* 1998; 193: 1–21.
56. Domogatskaya A, Rodin S and Tryggvason K. Functional diversity of laminins. *Annu Rev Cell Dev Biol* 2012; 28: 523–553.
57. Hohenester E and Yurchenco PD. Laminins in basement membrane assembly. *Cell Adh Migr* 2013; 7: 56–63.
58. Eckert RL, Crish JF, Efimova T, et al. Regulation of involucrin gene expression. *J Investig Dermatol* 2004; 123: 13–22.
59. Kim H, Shin JU and Lee KH. Atopic dermatitis and skin barrier dysfunction. *Allergy Asthma Respir Dis* 2013; 1: 20–28.
60. Baroni A, Buommino E, De Gregorio V, et al. Structure and function of the epidermis related to barrier properties. *Clin Dermatol* 2012; 30: 257–262.
61. Ganeshkumar M, Ponrasu T, Krithika R, et al. Topical application of Acalypha indica accelerates rat cutaneous wound healing by up-regulating the expression of type I and III collagen. *J Ethnopharmacol* 2012; 142(1): 14–22.
62. He Z, Ong CH, Halper J, et al. Progranulin is a mediator of the wound response. *Nat Med* 2003; 9(2): 225–229.
63. Cho J-W, Kang M-C and Lee K-S. TGF-β1-treated ADSCs-CM promotes expression of type I collagen and MMP-1, migration of human skin fibroblasts, and wound healing in vitro and in vivo. *Int J Mol Med* 2010; 26: 901–906.
64. Fu X, Xu M, Jia C, et al. Differential regulation of skin fibroblasts for their TGF-β1-dependent wound healing activities by biomimetic nanofibers. *J Mater Chem B* 2016; 4: 5246–5255.
65. Kipshidze N, Nikolaychik V, Keelan MH, et al. Low-power helium: neon laser irradiation enhances production of vascular endothelial growth factor and promotes growth of endothelial cells in vitro. *Lasers Surg Med* 2001; 28: 355–364.
66. Triana MA, Restrepo AA, Lanzafame RJ, et al. Quantum dot light-emitting diodes as light sources in photomedicine: photodynamic therapy and photobiomodulation. *J Phys Mater* 2020; 3: 032002.
67. Solmaz H, Ulgen Y and Gulsoy M. Photobiomodulation of wound healing via visible and infrared laser irradiation. *Lasers Med Sci* 2017; 32: 903–910.
68. Chen Z, Li W, Hu X, et al. Irradiance plays a significant role in photobiomodulation of B16F10 melanoma cells by increasing reactive oxygen species and inhibiting mitochondrial function. *Biomed Opt Express* 2019; 11: 27–39.
69. Lee G, Won H-S, Lee Y-M, et al. Oxidative dimerization of PHD2 is responsible for its inactivation and contributes to metabolic reprogramming via HIF-1α activation. *Sci Rep* 2016; 6: 18928.
70. Calvani M, Comito G, Giannoni E, et al. Time-dependent stabilization of hypoxia inducible factor-1α by different intracellular sources of reactive oxygen species. *PLoS One* 2012; 7: e38388.
71. Ikwegbue PC, Masamba P, Oyinloye BE, et al. Roles of heat shock proteins in apoptosis, oxidative stress, human inflammatory diseases, and cancer. *Pharmaceuticals* 2017; 11: 2.
72. Chatterjee S and Burns TF. Targeting heat shock proteins in cancer: a promising therapeutic approach. *Int J Mol Sci* 2017; 18: 1978.
73. Skora D and Gorska M. Heat shock proteins and their association with major pediatric malignancies. *Front Biosci* 2016; 21: 157–164.
74. Evangelista AN, Dos Santos FF, de Oliveira Martins LP, et al. Photobiomodulation therapy on expression of HSP70 protein and tissue repair in experimental acute Achilles tendinitis. *Lasers Med Sci* 2021; 36: 1201–1208.
75. Song Q, Uygun B, Banerjee I, et al. Low power laser irradiation stimulates the proliferation of adult human retinal pigment epithelial cells in culture. *Cell Mol Bioeng* 2009; 2: 87–103.
76. Castilho-Fernandes A, Lopes TG, Ferreira FU, et al. Adipogenic differentiation of murine bone marrow mesenchymal stem cells induced by visible light via photo-induced biomodulation. *Photodiagnosis Photodyn Ther* 2019; 25: 119–127.
77. Wang L, Wu F, Liu C, et al. Low-level laser irradiation modulates the proliferation and the osteogenic differentiation of bone marrow mesenchymal stem cells under healthy and inflammatory condition. *Lasers Med Sci* 2019; 34(1): 169–178.
78. Zamani ARN, Saberianpour S, Geranmayeh MH, et al. Modulatory effect of photobiomodulation on stem cell epigenetic memory: a highlight on differentiation capacity. *Lasers Med Sci* 2020; 35(2): 299–306.
79. Eduardo FDP, Bueno DF, de Freitas PM, et al. Stem cell proliferation under low intensity laser irradiation: a preliminary study. *Lasers Surg Med* 2008; 40: 433–438.
80. Pereira LO, Longo JP and Azevedo RB. Laser irradiation did not increase the proliferation or the differentiation of stem cells from normal and inflamed dental pulp. *Arch Oral Biol* 2012; 57: 1079–1085.
81. Tsai C-C, Su PF, Huang Y-F, et al. Oct4 and Nanog directly regulate Dnmt1 to maintain self-renewal and undifferentiated state in mesenchymal stem cells. *Mol Cell* 2012; 47: 169–182.
82. Kim MO, Kim S-H, Cho Y-Y, et al. ERK1 and ERK2 regulate embryonic stem cell self-renewal through phosphorylation of Klf4. *Nat Struct Mol Biol* 2012; 19: 283–290.
83. Zhang P, Andrianakos R, Yang Y, et al. Kruppel-like factor 4 (Klf4) prevents embryonic stem (ES) cell differentiation by regulating Nanog gene expression. *J Biol Chem* 2010; 285: 9180–9189.

84. Liao X, Xie G-H, Liu H-W, et al. Helium-neon laser irradiation promotes the proliferation and migration of human epidermal stem cells in vitro: proposed mechanism for enhanced wound re-epithelialization. *Photomed Laser Surg* 2014; 32: 219–225.
85. Newby AC. Matrix metalloproteinases regulate migration, proliferation, and death of vascular smooth muscle cells by degrading matrix and non-matrix substrates. *Cardiovasc Res* 2006; 69: 614–624.
86. Yu Q, Chen L, You Y, et al. Erythropoietin combined with granulocyte colony-stimulating factor enhances MMP-2 expression in mesenchymal stem cells and promotes cell migration. *Mol Med Rep* 2011; 4: 31–36.
87. Ayuk SM, Abrahamse H and Houreld NN. The role of matrix metalloproteinases in diabetic wound healing in relation to photobiomodulation. *J Diabetes Res* 2016; 2016: 2897656.
88. Lim WB, Kim JS, Ko YJ, et al. Effects of 635nm light-emitting diode irradiation on angiogenesis in $CoCl_2$-exposed HUVECs. *Lasers Surg Med* 2011; 43: 344–352.
89. Hirota K and Semenza GL. Regulation of angiogenesis by hypoxia-inducible factor 1. *Crit Rev Oncol Hematol* 2006; 59(1): 15–26.
90. Ryu JM, Lee HJ, Jung YH, et al. Regulation of stem cell fate by ROS-mediated alteration of metabolism. *Int J Stem Cells* 2015; 8: 24–35.
91. Yoshida K, Kirito K, Yongzhen H, et al. Thrombopoietin (TPO) regulates HIF-1alpha levels through generation of mitochondrial reactive oxygen species. *Int J Hematol* 2008; 88: 43–51.
92. Huang Y-J and Nan G-X. Oxidative stress-induced angiogenesis. *J Clin Neurosci* 2019; 63: 13–16.
93. Yoshimura A, Wakabayashi Y and Mori T. Cellular and molecular basis for the regulation of inflammation by TGF-β. *J Biochem* 2010; 147: 781–792.
94. Chang Z, Kishimoto Y, Hasan A, et al. TGF-β3 modulates the inflammatory environment and reduces scar formation following vocal fold mucosal injury in rats. *Dis Model Mech* 2013; 7: 83–91.
95. Prud'homme GJ. Pathobiology of transforming growth factor beta in cancer, fibrosis and immunologic disease, and therapeutic considerations. 2007; 87: 1077–1091.
96. Eriksen JL and Mackenzie IR. Progranulin: normal function and role in neurodegeneration. *J Neurochem* 2008; 104: 287–297.